REPORT

THE JOURNAL OF BIOLOGICAL CHEMISTRY VOL. 289, NO. 23, pp. 15980–15985, June 6, 2014


# Channel Formation by Yeast F-ATP Synthase and the Role of Dimerization in the Mitochondrial Permeability Transition*◆

Received for publication, February 19, 2014, and in revised form, April 18, 2014
Published, JBC Papers in Press, May 1, 2014, DOI 10.1074/jbc.C114.559633

**Michela Carraro**[‡1,2], **Valentina Giorgio**[‡1], **Justina Šileikytė**[‡], **Geppo Sartori**[‡], **Michael Forte**[§], **Giovanna Lippe**[¶], **Mario Zoratti**[‡], **Ildikò Szabò**[‖], **and Paolo Bernardi**[‡3]

*From the* [‡]*Consiglio Nazionale delle Ricerche Neuroscience Institute and Department of Biomedical Sciences and the* [‖]*Department of Biology, University of Padova, I-35121 Padova, Italy the* [§]*Vollum Institute, Oregon Health and Sciences University, Portland, Oregon 97239-3098, and the* [¶]*Department of Food Science, University of Udine, 33100 Udine, Italy*

**Background:** Whether channel formation is a general feature of F-ATP synthase dimers across species is unknown.
**Results:** Yeast F-ATP synthase dimers form $Ca^{2+}$-dependent channels, and the e and g subunits facilitate pore formation *in situ* through dimerization.
**Conclusion:** F-ATP synthase dimers form the permeability transition pore of yeast.
**Significance:** $Ca^{2+}$-dependent channel formation is a conserved feature of F-ATP synthases.

**Purified F-ATP synthase dimers of yeast mitochondria display $Ca^{2+}$-dependent channel activity with properties resembling those of the permeability transition pore (PTP) of mammals. After treatment with the $Ca^{2+}$ ionophore ETH129, which allows electrophoretic $Ca^{2+}$ uptake, isolated yeast mitochondria undergo inner membrane permeabilization due to PTP opening. Yeast mutant strains Δ*TIM11* and Δ*ATP20* (lacking the e and g F-ATP synthase subunits, respectively, which are necessary for dimer formation) display a striking resistance to PTP opening. These results show that the yeast PTP originates from F-ATP synthase and indicate that dimerization is required for pore formation *in situ*.**

Mitochondria from a variety of sources can undergo an inner membrane permeability increase, the permeability transition (PT),[4] due to opening of a high conductance channel, the PT pore (PTP) (1). The PTP coincides with the mitochondrial megachannel (MMC) defined by patch clamp studies in mitoplasts (2–5). In mammals, PTP opening requires matrix $Ca^{2+}$ and is favored by oxidative stress and $P_i$, inhibited by adenine nucleotides and $Mg^{2+}$, and antagonized by cyclosporin A (CsA) through its interaction with matrix cyclophilin (CyP)D (6, 7). The mammalian PTP is today recognized to play a role in cell death in a variety of disease paradigms (8).

Inner membrane permeability pathways have been described in yeast (9) and in *Drosophila melanogaster* (10), but whether these coincide with the mammalian PTP remains an open question (11–14). The issue is particularly complex in the case of yeast, where multiple conductance pathways may exist including an uncoupling protein-independent permeability activated by ATP (15–17). Furthermore, the yeast PTP (yPTP) is inhibited rather than activated by $P_i$ and insensitive to CsA (9), and due to the lack of a mitochondrial $Ca^{2+}$ uniporter, its $Ca^{2+}$ dependence has been more difficult to assess (18), although the $Ca^{2+}$ content of *Saccharomyces cerevisiae* mitochondria is close to that of rat liver mitochondria (19). The problem of the $Ca^{2+}$ dependence was solved by the Shinohara group (20), who showed that yeast mitochondria incubated with optimized substrate and $P_i$ concentrations readily undergo a $Ca^{2+}$-dependent PT upon treatment with ETH129, a $Ca^{2+}$ ionophore that allows electrophoretic $Ca^{2+}$ transport into the matrix of energized mitochondria. We recently demonstrated that dimers of mammalian F-ATP synthase reconstituted into planar bilayers give rise to $Ca^{2+}$-activated currents with conductances ranging up to 1.3 nS in 150 mM KCl that closely match those displayed by the MMC-PTP (21). Here we have tested whether gel-purified F-ATP synthase dimers of *S. cerevisiae* form channels when reconstituted in lipid bilayers, and whether dimerization of the F-ATP synthase is necessary for PTP formation in intact mitochondria.

## EXPERIMENTAL PROCEDURES

*Yeast Strains and Materials*—The *S. cerevisiae* strains BY4743 (4741/4742), as well as the mutants Δ*CPR3* (MATa, *his3Δ1*, *leu2Δ0*, *met5Δ0*, *ura3Δ0*), Δ*TIM11* (MATa, *his3Δ1*, *leu2Δ0*, *met5Δ0*, *ura3Δ0*), and Δ*ATP20* (MATα, *his3Δ1*, *leu2Δ0*, *lys2Δ0*, *ura3Δ0*), were purchased from Thermo Scientific. Δ*TIM11*Δ*ATP20* mutants were obtained by mating the Δ*TIM11* and Δ*ATP20* strains and selecting the formed diploid by growth on synthetic defined (0.67% nitrogen base without amino acids, 2% dextrose) selective medium containing the

* This work was supported in part by Associazione Italiana per la Ricerca sul Cancro (AIRC) Grants IG13392 (to P. B.) and IG11814 (to I. S.), Progetti di Ricerca di Interesse Nazionale Programs 20107Z8XBW (to P. B.) and 2010CSJX4F (to I. S.), National Institutes of Health/Public Health Service Grant 1R01GM069883 (to M. F. and P. B.), a Consiglio Nazionale delle Ricerche (CNR) Project of Special Interest on Aging (to M. Z.), and the University of Padova Progetti Strategici di Ateneo "Models of Mitochondrial Diseases" (to P. B.).
◆ This article was selected as a Paper of the Week.
[1] Both authors contributed equally to this work.
[2] This work is in partial fulfillment of the requirements for a Ph.D. at the University of Padova.
[3] To whom correspondence should be addressed: Dept. of Biomedical Sciences, University of Padova, Via Ugo Bassi 58/B, I-35121 Padova, Italy. Fax: 39-049-827-6049; E-mail: bernardi@bio.unipd.it.

[4] The abbreviations used are: PT, permeability transition; PTP, permeability transition pore; yPTP, yeast permeability transition pore; BN-PAGE, blue native polyacrylamide gel electrophoresis; CRC, $Ca^{2+}$ retention capacity; $Cu(OP)_2$, copper-*o*-phenanthroline; CsA, cyclosporin A; CyPD, cyclophilin D; MMC, mitochondrial megachannel; PhAsO, phenylarsine oxide; Tricine, *N*-[2-hydroxy-1,1-bis(hydroxymethyl)ethyl]glycine; Bis-Tris, 2-(bis(2-hydroxyethyl)amino)-2-(hydroxymethyl)propane-1,3-diol; S, siemens.

required nutritional supplements except methionine and lysine. Diploids were then induced to sporulate in 1% potassium acetate, tetrads were dissected, and haploids were analyzed with semiquantitative PCR to detect null mutants for *TIM11* and *ATP20* genes. Digitonin was from Sigma, and ETH129 was from Sigma-Aldrich Japan and was dissolved in methanol. NADH, disodium salt was purchased from Roche Applied Science.

*Yeast Culture and Mitochondria Isolation*—Yeast cells were cultured aerobically in 50 ml of 1% yeast extract, 1% bacto-polypeptone medium containing 2% glucose at 30 °C. When it reached an optical density of 2 at 600 nm, the culture was added to 800 ml of bacto-polypeptone medium supplemented with 2% galactose and incubated for 20 h at 30 °C under rotation at 180 rpm, yielding about 4.0 g of yeast cells. Yeast mitochondria were isolated as described (20) with the following modifications. Briefly, cells were washed, incubated for 15 min at 37 °C in a 0.1 M Tris-$SO_4$ buffer (pH 9.4) supplemented with 10 mM dithiothreitol (DTT), and washed once with 1.2 M sorbitol, 20 mM $P_i$, pH 7.4. Yeast cells were then suspended in the same buffer and incubated for 45 min at 30 °C with 0.4 mg/g of cells of Zymolyase 100T to form spheroplasts. The latter were washed once with sorbitol buffer and homogenized in 0.6 M Mannitol, 10 mM Tris-HCl, pH 7.4, and 0.1 mM EDTA-Tris with a Potter homogenizer. The homogenate was centrifuged for 5 min at 2,000 × *g*, and the supernatant was collected and centrifuged for 10 min at 12,000 × *g*. The resulting mitochondrial pellet was suspended in mannitol buffer, and protein concentration was determined from the $A_{280}$ of SDS-solubilized mitochondria (14).

*Mitochondrial Calcium Retention Capacity*—Mitochondrial $Ca^{2+}$ uptake was measured with Calcium Green-5N (Molecular Probes) fluorescence using a Fluoroskan Ascent FL (Thermo Electron) plate reader at a mitochondrial concentration of 0.5 mg × $ml^{-1}$. Mitochondria were incubated as specified in the figure legends.

*Gel Electrophoresis and Western Blotting*—Mitochondria were suspended at 10 mg/ml in 150 mM potassium acetate, 30 mM HEPES, 10% glycerol, 1 mM phenylmethylsulfonyl fluoride and solubilized with 1.5% (w/v) digitonin. After centrifugation at 100,000 × *g* with a Beckman TL-100 rotor for 25 min at 4 °C, supernatants were collected, supplemented with 50 mg/ml Coomassie Blue and 5 M aminocaproic acid, and quickly loaded onto a blue native polyacrylamide 3–12% gradient gel (BN-PAGE, Invitrogen). Electrophoresis was carried out at 150 V for 20 min and at 250 V for 2 h followed by gel staining with 0.25 mg/ml Coomassie Blue, 10% acetic acid or used for in-gel activity staining to detect bands corresponding to ATP synthase. Activity was monitored in 270 mM glycine, 35 mM Tris, pH 7.4, 15 mM $MgSO_4$, 8 mM ATP, Tris-buffered to pH 7.4, and 2 mg/ml $Pb(NO_3)_2$. Bands corresponding to monomeric and dimeric forms of ATP synthase were cut from the gels, and protein complexes were eluted overnight by incubation at 4 °C in 25 mM Tricine, 15 mM $MgSO_4$, 8 mM ATP, 7.5 mM Bis-Tris, 1% (w/v) *n*-heptyl β-D-thioglucopyranoside, pH 7.0. Samples were then centrifuged at 20,000 × *g* for 10 min at 4 °C, and supernatants were used for bilayer experiments. For cross-linking experiments, mitochondria were incubated 20 min at room temperature at 1 mg/ml in 250 mM sucrose, 2 mM $P_i$, and 2 mM $CuCl_2$. Five millimolar *N*-ethylmaleimide and 5 mM EDTA were then added to block the cross-linking reaction, and the incubations were transferred on ice for 10 min followed by centrifugation and preparation for BN-PAGE as described above. Total yeast mitochondria lysates and bands corresponding to dimers of F-ATP synthase cut out of BN-PAGE gels were subjected to SDS-PAGE followed by silver staining or transfer to nitrocellulose for Western blot analysis. Antibodies were polyclonal rabbit anti-ATP synthase γ subunit (a gift from Marie-France Giraud, Bordeaux, France), anti-Tom20 and anti-Tim54 (a gift from Nikolaus Pfanner, Freiburg, Germany).

*Electrophysiology*—Planar lipid bilayer experiments were performed as described in Ref. 31. Briefly, bilayers of 150–200 picofarads of capacitance were prepared using purified soybean asolectin. The standard experimental medium was 150 mM KCl, 10 mM Hepes, pH 7.5. All reported voltages refer to the *cis* chamber, zero being assigned to the *trans* (grounded) side. Currents are considered as positive when carried by cations flowing from the *cis* to the *trans* compartment. Freshly prepared F-ATP synthase dimers were added to the *cis* side. No current was observed when PTP activators were added to the membrane in the absence of F-ATP synthase dimers ($n = 2$).

## RESULTS AND DISCUSSION

*Properties of the $Ca^{2+}$-dependent Permeability Transition of Yeast Mitochondria*—We used ETH129 to allow $Ca^{2+}$ uptake by energized yeast mitochondria (20) and monitored the propensity of the yPTP to open based on the $Ca^{2+}$ retention capacity (CRC), *i.e.* the maximal $Ca^{2+}$ load retained by mitochondria before onset of the PT (22). In keeping with previous observations (20), (i) energized yeast mitochondria were able to accumulate $Ca^{2+}$ provided as a train of pulses (Fig. 1*A*) until onset of the PT, which causes depolarization followed by $Ca^{2+}$ release; and (ii) increasing concentrations of $P_i$ increased the matrix $Ca^{2+}$ load necessary to open the yPTP (Fig. 1, *A* and *B*), possibly following formation of matrix $P_i$-$Ca^{2+}$ complexes. As in mammalian mitochondria, $Mg^{2+}$-ADP increased the CRC, an effect consistent with yPTP inhibition (Fig. 1*C*). The CRC was not affected by decavanadate (results not shown), which inhibits the ATP-induced, voltage-dependent anion channel (VDAC)-dependent yeast permeability pathway (23, 24).

The mammalian PTP is modulated by two classes of redox-sensitive thiols whose oxidation increases the pore sensitivity to $Ca^{2+}$, *i.e.* (i) matrix thiols that react with phenylarsine oxide (PhAsO) and can be oxidized by diamide (25); and (ii) external thiols that can be oxidized by copper-*o*-phenanthroline ($Cu(OP)_2$) (26). The threshold $Ca^{2+}$ load required for yPTP opening was moderately affected by PhAsO (Fig. 1*D*), whereas it was very sensitive to diamide (Fig. 1*E*) and to $Cu(OP)_2$ (Fig. 1*F*). These experiments indicate that the yeast PTP is affected by the redox state of thiol groups as also suggested by a previous study (18).

CsA desensitizes the mammalian pore to $Ca^{2+}$ through matrix CyPD, a peptidyl-prolyl *cis-trans* isomerase that behaves as a PTP inducer (27, 28). Through studies of CyPD-null mitochondria, it became clear that CyPD is a modulator but not an obligatory constituent of the PTP and that a PT can occur in the

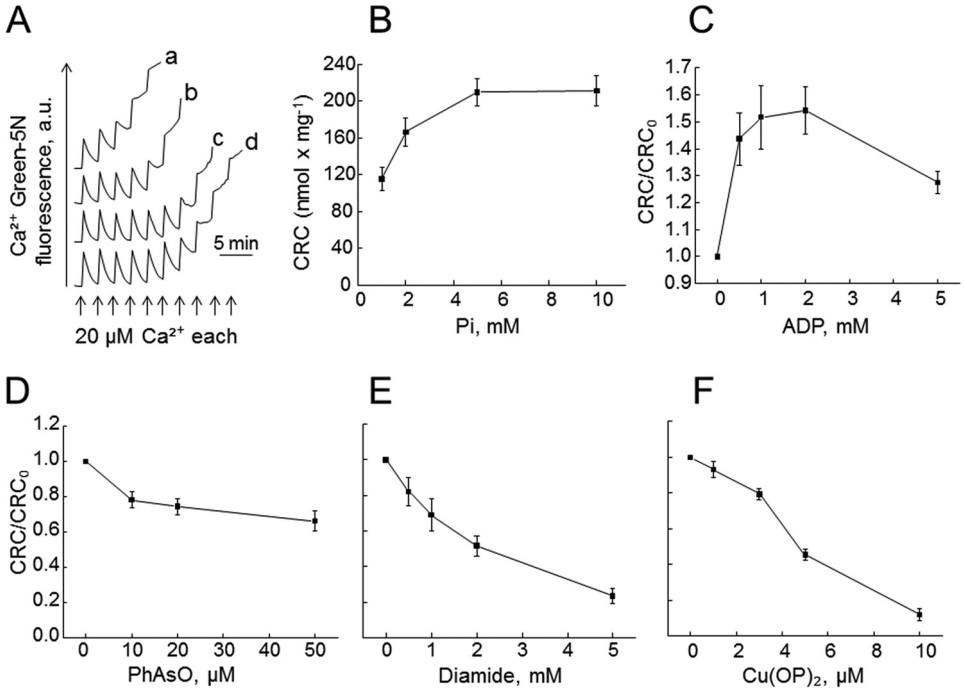


FIGURE 1. **Properties of the permeability transition of yeast mitochondria.** The incubation medium contained 250 mM sucrose, 10 mM Tris-MOPS, 1 mM NADH, 10 $\mu$M EGTA-Tris, 5 $\mu$M ETH129, 1 $\mu$M Calcium Green-5N, final pH 7.4, 0.5 mg/ml bovine serum albumin, and 0.1 mg of mitochondria in a final volume of 0.2 ml. *A*, the medium was supplemented with 1 mM (*trace a*), 2 mM (*trace b*), 5 mM (*trace c*), or 10 mM $P_i$ (*trace d*), and where indicated, $Ca^{2+}$ was added. Traces shown are representative of 13 independent experiments. *a.u.*, arbitrary units. *B*, experimental conditions as in *panel A* with the indicated $P_i$ concentrations. Values on the ordinate refer to the amount of $Ca^{2+}$ accumulated prior to the precipitous release that follows the PT ($n = 13 \pm$ S.E.). *C*, the experimental conditions were as in *panel A* with 2 mM $P_i$, and the medium was supplemented with 2 mM $MgCl_2$, 1 $\mu$M oligomycin, and the stated concentrations of ADP ($n = 8 \pm$ S.E.). *D–F*, the experimental conditions were as in *panel A* with 2 mM $P_i$, and the medium was supplemented with the stated concentrations of PhAsO (*D*), diamide (*E*), or $Cu(OP)_2$ (*F*). For *panels D–F*, *n* ($\pm$ S.E.) was 6, 4, and 7, respectively.

absence of CyPD, or in the presence of CsA, albeit at higher matrix $Ca^{2+}$ loads (8). Yeast mitochondria possess a matrix CyP (CPR3), which facilitates folding of imported proteins in the matrix and is sensitive to CsA (29); however, the yPTP is not affected by CsA (9), as also confirmed in the CRC assay (Fig. 2*A*, compare *traces a* and *b*). These findings suggest either that CPR3 does not interact with the pore or that CsA does not interfere with CPR3 binding. To resolve this issue, we tested the CRC of Δ*CPR3* mutants, which displayed a lower rate and slightly lower extent of $Ca^{2+}$ accumulation (Fig. 2*A*, *trace c*), indicating that CPR3 does not sensitize the yPTP to $Ca^{2+}$, at variance from the effects of CyPD in mammalian mitochondria (30). The small decrease of CRC in the mutants (Fig. 2*B*) may be due to slower protein import and defective respiratory chain assembly and/or function (31). It was recently established that rotenone is a good inhibitor of the PTP in mammalian mitochondria lacking CyPD, possibly because of decreased production of reactive oxygen species through inhibition of reverse electron flow (32). Rotenone did not affect the yPTP (Fig. 2*A*, *trace d*), in keeping with the lack of a rotenone-sensitive, energy-conserving complex I and with the lack of "off-site" effects. Taken together, the above results suggest that, despite the lack of a fast $Ca^{2+}$ uptake system (19), *S. cerevisiae* mitochondria can undergo a $Ca^{2+}$-induced PT, which displays some similarities with the mammalian PT (sensitization by matrix $Ca^{2+}$ and oxidative stress, inhibition by $Mg^{2+}$-ADP), but also some differences (inhibition by phosphate and lack of sensitivity to CPR3 and rotenone).

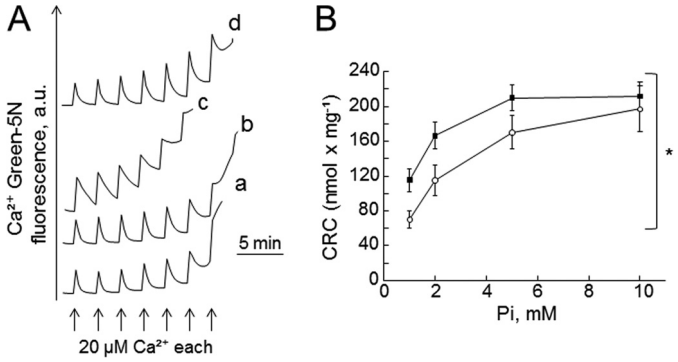


FIGURE 2. ***CPR3* deletion does not affect the yeast permeability transition.** *A*, the experimental conditions were as in Fig. 1 with 2 mM $P_i$; 0.8 $\mu$M CsA was added in *trace b* only, and 2 $\mu$M rotenone was added in *trace d* only. Where indicated, $Ca^{2+}$ was added to wild-type (*traces a*, *b*, and *d*) or Δ*CPR3* (*trace c*) mitochondria (traces are representative of three independent experiments). *B*, the experimental conditions were as in Fig. 1 with $P_i$ as indicated ($n = 4 \pm$ S.E.). *Closed symbols*, wild-type mitochondria; *open symbols*, Δ*CPR3* mitochondria. Two-way analysis of variance test was performed, *, $p < 0.05$.

*Purified F-ATP Synthase Dimers Possess Channel Activity*—To test whether yeast F-ATP synthase dimers can form channels similar to those found in mammals (21), we separated mitochondrial protein extracts by BN-PAGE, identified dimers by in-gel activity staining, and eluted them for incorporation into a planar asolectin membrane (see Fig. 4*A* for an example of the dimer used). The addition of 1–10 pmol of the dimers to the bilayers in symmetrical 150 mM KCl did not elicit current activity unless $Ca^{2+}$, PhAsO, and $Cu(OP)_2$ were also added (Fig. 3*A*). We observed a clear activity in 12 out of 14 reconstitutions, with

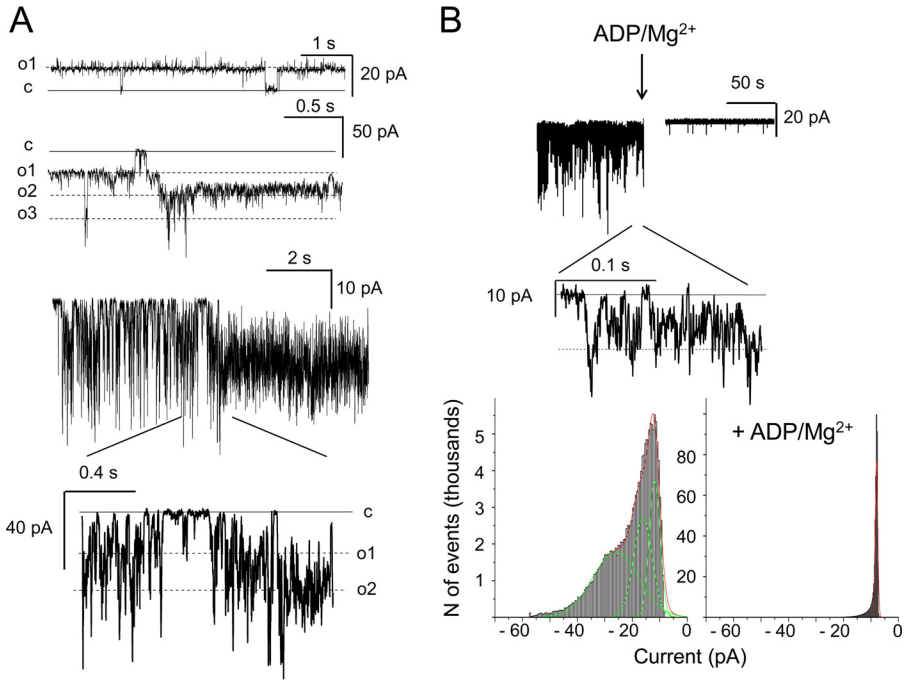


FIGURE 3. **F-ATP synthase dimers reconstituted in planar lipid bilayers display $Ca^{2+}$-induced currents.** Dimers were excised (see Fig. 4*A*, wild-type) and eluted for planar bilayer experiments. *A*, *upper part*, representative current traces recorded at +80 and −100 mV (*cis*) (*upper* and *lower traces*, conductance (g) = 125 and 250 pS) upon incorporation of purified dimeric F-ATP synthase following the addition of 3 mM $Ca^{2+}$ (added to the *trans* side) plus 0.1 mM PhAsO and 20 $\mu$M $Cu(OP)_2$ (added to both sides). *Lower part*, typical, most often observed channel kinetics (see also expanded portion of the recording obtained at −60 mV (*cis*); g = 250 pS). *a.u.*, arbitrary units. *B*, *top*, effect of 2 mM ADP plus 1.6 mM $Mg^{2+}$ added to the *trans* side on channel activity (−60 mV, g = 250 pS); current trace before and immediately after the addition of the modulators is shown. *Bottom*, amplitude histograms obtained from the same experiment before (*left panel*) and after (*right panel*) the addition of ADP/$Mg^{2+}$. Gaussian fitting (*green lines*) was obtained using the Origin 6.1 Program Set.

channel unit conductance usually ranging between 250 and 300 pS (multiples of this unit conductance were often observed; in one case 1000 pS was reached). This conductance is compatible with the values exhibited by a channel observed in mitoplasts from a porin-less yeast strain, which was insensitive to CsA, ADP, or protons and in which the combination of ADP and $Mg^{2+}$ was not tested (33). The activity studied here was characterized by rapid oscillations between closed and open states (flickering), which is typical of the mammalian MMC-PTP, and by variable kinetics. A typical flickering behavior is illustrated in the bottom part of Fig. 3*A*. As is the case for the mammalian F-ATP synthase (21) and for the MMC-PTP measured in mitoplasts (4), the addition of $Mg^{2+}$-ADP induced a clear-cut inhibition of the channel in five out of six experiments (total inhibition was observed in two cases, and partial inhibition was observed in three cases). The representative experiment of Fig. 3*B* shows activity recorded before and immediately after the addition of $Mg^{2+}$-ADP in one case of full inhibition, which is illustrated in the corresponding amplitude histograms (Fig. 3*B*). Taken together, these data provide evidence that under conditions of oxidative stress, yeast F-ATP synthase can form $Ca^{2+}$-activated channels with features resembling the MMC-PTP (although with lower conductance). It should be noted that the dimer preparation did not contain Tom20 or Tim54 (Fig. 4*A*) and therefore that channel activity cannot be due to the twin pore translocase (34).

*Dimerization of F-ATP Synthase Is Required for PTP Formation*—Dimers of F-ATP synthase are the "building blocks" of long rows of oligomers located deep into the cristae, which contribute to formation of membrane curvature and to maintenance of proper cristae shape and mitochondrial morphology (35–42). Mammalian F-ATP synthase dimers also appear to be the units from which the PTP forms in a process that is highly favored by $Ca^{2+}$ and oxidative stress (21), events that are required for channel formation (8, 21). To test the hypothesis that yPTP formation requires the presence of F-ATP synthase dimers, we studied mutants lacking subunits involved in dimerization/oligomerization of the enzyme, *i.e.* subunit e (TIM11) and subunit g (ATP20) (35, 43–45). Strains lacking these subunits display balloon-shaped cristae with ATP synthase monomers distributed randomly in the membrane (39). The Δ*TIM11*, Δ*ATP20*, and Δ*TIM11*Δ*ATP20* mutants lacked dimers when analyzed by BN-PAGE, whereas the monomeric F-ATP synthase was assembled and active (Fig. 4*A*), consistent with their ability to grow on non-fermentable carbon sources, and developed a normal membrane potential upon energization with NADH (results not shown). CRC assays with ETH129 demonstrated that mitochondria from Δ*TIM11*, Δ*ATP20*, and Δ*TIM11*Δ*ATP20* strains take up a larger $Ca^{2+}$ load than wild-type strains (Fig. 4*B*), with a doubling of the CRC (Fig. 4*C*).

Dimers may transiently form also in Δ*TIM11* and Δ*ATP20* strains (46), a finding that could explain why $Ca^{2+}$ release is eventually observed also in the "dimerization-less" mutants. Consistent with this possibility, we did detect dimers in BN-PAGE after treatment with $CuCl_2$ (Fig. 4*D*), which promotes formation of disulfide bridges between adjacent cysteine residues of the monomers (45, 47, 48). Not all of the monomers dimerized after $CuCl_2$ treatment (Fig. 4*D*), suggesting that cysteine oxidation stabilizes pre-existing dimers that are otherwise

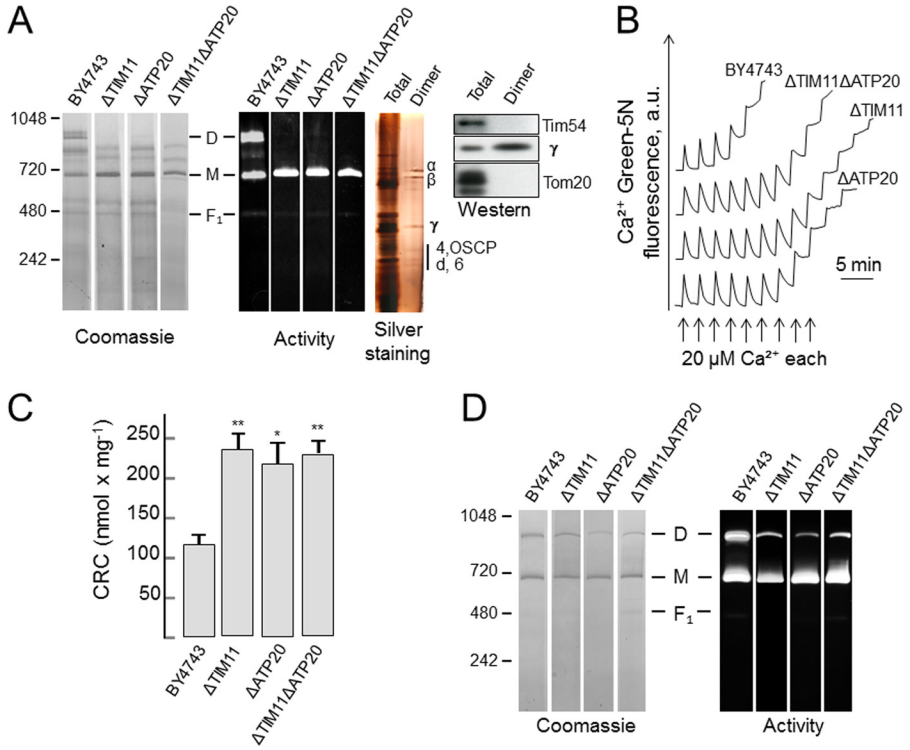


FIGURE 4. **Δ*TIM11*, Δ*ATP20*, and Δ*TIM11*Δ*ATP20* mutants lacking subunits involved in dimerization of F-ATP synthase are resistant to PTP opening.** *A*, mitochondrial protein extracts were separated with BN-PAGE and stained with Coomassie blue (lanes labeled *Coomassie*) or subjected to in-gel activity staining (lanes labeled *Activity*) to identify bands of F-ATP synthase dimers (*D*) and monomers (*M*) (note also a faint band corresponding to $F_1$ ($F^1$)). The gel region corresponding to the dimers of the BY4743 strain was cut out and subjected to SDS-PAGE together with a mitochondrial extract from the same strain followed by silver staining (lanes labeled *Silver staining*) or blotting and probing with the indicated antibodies (lanes labeled *Western*). OSCP, oligomycin sensitivity-conferring protein. *B*, the experimental conditions were as in Fig. 1 with 1 mM $P_i$. Where indicated, $Ca^{2+}$ was added to wild type, Δ*TIM11*Δ*ATP20*, Δ*TIM11*, or Δ*ATP20* mutants (traces are representative of 13, 6, 7, and 6 independent experiments for the corresponding genotypes). *C*, experimental conditions as in *A* with 1 mM $P_i$. One-way analysis of variance test was performed to analyze CRC differences between BY4743 and mutants, *, $p < 0.01$, **, $p < 0.001$. *D*, BN-PAGE (*left lanes*) and activity staining (*right lanes*) of mitochondria with the indicated genotypes after treatment with 2 mM $CuCl_2$.

dissociated by detergent treatment, but does not *induce* cross-linking of monomers.

In summary, our data provide the first demonstration that yeast F-ATP synthase dimers form high conductance channels analogous to the mammalian MMC-PTP, and thus that channel formation is a conserved feature of F-ATP synthases; show that yeast mitochondria can undergo a *bona fide* PT activated by oxidative stress; and indicate that dimers of F-ATP synthase are required for PTP formation *in situ* (21). Our findings do not exclude the existence of other permeability pathways that may involve the voltage-dependent anion channel (23, 24), nor the possible regulation of yPTP by outer mitochondrial membrane proteins (8). We think that it will now be possible to unravel the many open questions about the structure and function of the PTP (8) with the powerful methods of yeast genetics.

*Acknowledgments—We thank Marie-France Giraud and Nikolaus Pfanner for the generous gift of antibodies and Raffaele Lopreiato for advice on the preparation of mutants.*

## REFERENCES

1. Hunter, D. R., Haworth, R. A., and Southard, J. H. (1976) Relationship between configuration, function, and permeability in calcium-treated mitochondria. *J. Biol. Chem.* **251,** 5069–5077
2. Kinnally, K. W., Campo, M. L., and Tedeschi, H. (1989) Mitochondrial channel activity studied by patch-clamping mitoplasts. *J. Bioenerg. Biomembr.* **21,** 497–506
3. Petronilli, V., Szabó, I., and Zoratti, M. (1989) The inner mitochondrial membrane contains ion-conducting channels similar to those found in bacteria. *FEBS Lett.* **259,** 137–143
4. Szabó, I., Bernardi, P., and Zoratti, M. (1992) Modulation of the mitochondrial megachannel by divalent cations and protons. *J. Biol. Chem.* **267,** 2940–2946
5. Szabó, I., and Zoratti, M. (1992) The mitochondrial megachannel is the permeability transition pore. *J. Bioenerg. Biomembr.* **24,** 111–117
6. Fournier, N., Ducet, G., and Crevat, A. (1987) Action of cyclosporine on mitochondrial calcium fluxes. *J. Bioenerg. Biomembr.* **19,** 297–303
7. Crompton, M., Ellinger, H., and Costi, A. (1988) Inhibition by cyclosporin A of a $Ca^{2+}$-dependent pore in heart mitochondria activated by inorganic phosphate and oxidative stress. *Biochem. J.* **255,** 357–360
8. Bernardi, P. (2013) The mitochondrial permeability transition pore: A mystery solved? *Front. Physiol.* **4,** 95
9. Jung, D. W., Bradshaw, P. C., and Pfeiffer, D. R. (1997) Properties of a cyclosporin-insensitive permeability transition pore in yeast mitochondria. *J. Biol. Chem.* **272,** 21104–21112
10. von Stockum, S., Basso, E., Petronilli, V., Sabatelli, P., Forte, M. A., and Bernardi, P. (2011) Properties of $Ca^{2+}$ transport in mitochondria of *Drosophila melanogaster*. *J. Biol. Chem.* **286,** 41163–41170
11. Manon, S., Roucou, X., Guérin, M., Rigoulet, M., and Guérin, B. (1998) Characterization of the yeast mitochondria unselective channel: a counterpart to the mammalian permeability transition pore? *J. Bioenerg. Biomembr.* **30,** 419–429
12. Azzolin, L., von Stockum, S., Basso, E., Petronilli, V., Forte, M. A., and Bernardi, P. (2010) The mitochondrial permeability transition from yeast to mammals. *FEBS Lett.* **584,** 2504–2509
13. Uribe-Carvajal, S., Luévano-Martínez, L. A., Guerrero-Castillo, S., Ca-

brera-Orefice, A., Corona-de-la-Peña, N. A., and Gutiérrez-Aguilar, M. (2011) Mitochondrial unselective channels throughout the eukaryotic domain. *Mitochondrion* **11,** 382–390
14. Bradshaw, P. C., and Pfeiffer, D. R. (2013) Characterization of the respiration-induced yeast mitochondrial permeability transition pore. *Yeast* **30,** 471–483
15. Prieto, S., Bouillaud, F., Ricquier, D., and Rial, E. (1992) Activation by ATP of a proton-conducting pathway in yeast mitochondria. *Eur. J. Biochem.* **208,** 487–491
16. Prieto, S., Bouillaud, F., and Rial, E. (1995) The mechanism for the ATP-induced uncoupling of respiration in mitochondria of the yeast *Saccharomyces cerevisiae*. *Biochem. J.* **307,** 657–661
17. Prieto, S., Bouillaud, F., and Rial, E. (1996) The nature and regulation of the ATP-induced anion permeability in *Saccharomyces cerevisiae* mitochondria. *Arch. Biochem. Biophys.* **334,** 43–49
18. Kowaltowski, A. J., Vercesi, A. E., Rhee, S. G., and Netto, L. E. (2000) Catalases and thioredoxin peroxidase protect *Saccharomyces cerevisiae* against $Ca^{2+}$-induced mitochondrial membrane permeabilization and cell death. *FEBS Lett.* **473,** 177–182
19. Carafoli, E., and Lehninger, A. L. (1971) A survey of the interaction of calcium ions with mitochondria from different tissues and species. *Biochem. J.* **122,** 681–690
20. Yamada, A., Yamamoto, T., Yoshimura, Y., Gouda, S., Kawashima, S., Yamazaki, N., Yamashita, K., Kataoka, M., Nagata, T., Terada, H., Pfeiffer, D. R., and Shinohara, Y. (2009) $Ca^{2+}$-induced permeability transition can be observed even in yeast mitochondria under optimized experimental conditions. *Biochim. Biophys. Acta* **1787,** 1486–1491
21. Giorgio, V., von Stockum, S., Antoniel, M., Fabbro, A., Fogolari, F., Forte, M., Glick, G. D., Petronilli, V., Zoratti, M., Szabó, I., Lippe, G., and Bernardi, P. (2013) Dimers of mitochondrial ATP synthase form the permeability transition pore. *Proc. Natl. Acad. Sci. U.S.A.* **110,** 5887–5892
22. Fontaine, E., Ichas, F., and Bernardi, P. (1998) A ubiquinone-binding site regulates the mitochondrial permeability transition pore. *J. Biol. Chem.* **273,** 25734–25740
23. Roucou, X., Manon, S., and Guérin, M. (1997) Conditions allowing different states of ATP- and GDP-induced permeability in mitochondria from different strains of *Saccharomyces cerevisiae*. *Biochim. Biophys. Acta* **1324,** 120–132
24. Gutiérrez-Aguilar, M., Pérez-Vázquez, V., Bunoust, O., Manon, S., Rigoulet, M., and Uribe, S. (2007) In yeast, $Ca^{2+}$ and octylguanidine interact with porin (VDAC) preventing the mitochondrial permeability transition. *Biochim. Biophys. Acta* **1767,** 1245–1251
25. Petronilli, V., Costantini, P., Scorrano, L., Colonna, R., Passamonti, S., and Bernardi, P. (1994) The voltage sensor of the mitochondrial permeability transition pore is tuned by the oxidation-reduction state of vicinal thiols: increase of the gating potential by oxidants and its reversal by reducing agents. *J. Biol. Chem.* **269,** 16638–16642
26. Costantini, P., Colonna, R., and Bernardi, P. (1998) Induction of the mitochondrial permeability transition by *N*-ethylmaleimide depends on secondary oxidation of critical thiol groups: potentiation by copper-*ortho*-phenanthroline without dimerization of the adenine nucleotide translocase. *Biochim. Biophys. Acta* **1365,** 385–392
27. Halestrap, A. P., and Davidson, A. M. (1990) Inhibition of $Ca^{2+}$-induced large-amplitude swelling of liver and heart mitochondria by cyclosporin is probably caused by the inhibitor binding to mitochondrial-matrix peptidyl-prolyl *cis-trans* isomerase and preventing it interacting with the adenine nucleotide translocase. *Biochem. J.* **268,** 153–160
28. Woodfield, K. Y., Price, N. T., and Halestrap, A. P. (1997) cDNA cloning of rat mitochondrial cyclophilin. *Biochim. Biophys. Acta* **1351,** 27–30
29. Matouschek, A., Rospert, S., Schmid, K., Glick, B. S., and Schatz, G. (1995) Cyclophilin catalyzes protein folding in yeast mitochondria. *Proc. Natl. Acad. Sci. U.S.A.* **92,** 6319–6323
30. Basso, E., Fante, L., Fowlkes, J., Petronilli, V., Forte, M. A., and Bernardi, P. (2005) Properties of the permeability transition pore in mitochondria devoid of Cyclophilin D. *J. Biol. Chem.* **280,** 18558–18561
31. Rassow, J., Mohrs, K., Koidl, S., Barthelmess, I. B., Pfanner, N., and Tropschug, M. (1995) Cyclophilin 20 is involved in mitochondrial protein folding in cooperation with molecular chaperones Hsp70 and Hsp60. *Mol. Cell. Biol.* **15,** 2654–2662
32. Li, B., Chauvin, C., De Paulis, D., De Oliveira, F., Gharib, A., Vial, G., Lablanche, S., Leverve, X., Bernardi, P., Ovize, M., and Fontaine, E. (2012) Inhibition of complex I regulates the mitochondrial permeability transition through a phosphate-sensitive inhibitory site masked by cyclophilin D. *Biochim. Biophys. Acta* **1817,** 1628–1634
33. Szabó, I., Báthori, G., Wolff, D., Starc, T., Cola, C., and Zoratti, M. (1995) The high-conductance channel of porin-less yeast mitochondria. *Biochim. Biophys. Acta* **1235,** 115–125
34. Rehling, P., Model, K., Brandner, K., Kovermann, P., Sickmann, A., Meyer, H. E., Kühlbrandt, W., Wagner, R., Truscott, K. N., and Pfanner, N. (2003) Protein insertion into the mitochondrial inner membrane by a twin-pore translocase. *Science* **299,** 1747–1751
35. Paumard, P., Vaillier, J., Coulary, B., Schaeffer, J., Soubannier, V., Mueller, D. M., Brèthes, D., di Rago, J.-P., and Velours, J. (2002) The ATP synthase is involved in generating mitochondrial cristae morphology. *EMBO J.* **21,** 221–230
36. Dudkina, N. V., Sunderhaus, S., Braun, H. P., and Boekema, E. J. (2006) Characterization of dimeric ATP synthase and cristae membrane ultrastructure from *Saccharomyces* and *Polytomella* mitochondria. *FEBS Lett.* **580,** 3427–3432
37. Strauss, M., Hofhaus, G., Schröder, R. R., and Kühlbrandt, W. (2008) Dimer ribbons of ATP synthase shape the inner mitochondrial membrane. *EMBO J.* **27,** 1154–1160
38. Thomas, D., Bron, P., Weimann, T., Dautant, A., Giraud, M. F., Paumard, P., Salin, B., Cavalier, A., Velours, J., and Brèthes, D. (2008) Supramolecular organization of the yeast $F_1F^o$-ATP synthase. *Biol. Cell* **100,** 591–601
39. Davies, K. M., Anselmi, C., Wittig, I., Faraldo-Gómez, J. D., and Kühlbrandt, W. (2012) Structure of the yeast $F_1F_o$-ATP synthase dimer and its role in shaping the mitochondrial cristae. *Proc. Natl. Acad. Sci. U.S.A.* **109,** 13602–13607
40. Davies, K. M., Strauss, M., Daum, B., Kief, J. H., Osiewacz, H. D., Rycovska, A., Zickermann, V., and Kühlbrandt, W. (2011) Macromolecular organization of ATP synthase and complex I in whole mitochondria. *Proc. Natl. Acad. Sci. U.S.A.* **108,** 14121–14126
41. Baker, L. A., Watt, I. N., Runswick, M. J., Walker, J. E., and Rubinstein, J. L. (2012) Arrangement of subunits in intact mammalian mitochondrial ATP synthase determined by cryo-EM. *Proc. Natl. Acad. Sci. U.S.A.* **109,** 11675–11680
42. Daum, B., Walter, A., Horst, A., Osiewacz, H. D., and Kühlbrandt, W. (2013) Age-dependent dissociation of ATP synthase dimers and loss of inner-membrane cristae in mitochondria. *Proc. Natl. Acad. Sci. U.S.A.* **110,** 15301–15306
43. Arnold, I., Pfeiffer, K., Neupert, W., Stuart, R. A., and Schägger, H. (1998) Yeast mitochondrial $F_1F_0$-ATP synthase exists as a dimer: identification of three dimer-specific subunits. *EMBO J.* **17,** 7170–7178
44. Wittig, I., Velours, J., Stuart, R., and Schägger, H. (2008) Characterization of domain interfaces in monomeric and dimeric ATP synthase. *Mol. Cell. Proteomics* **7,** 995–1004
45. Habersetzer, J., Ziani, W., Larrieu, I., Stines-Chaumeil, C., Giraud, M. F., Brèthes, D., Dautant, A., and Paumard, P. (2013) ATP synthase oligomerization: from the enzyme models to the mitochondrial morphology. *Int. J. Biochem. Cell Biol.* **45,** 99–105
46. Gavin, P. D., Prescott, M., and Devenish, R. J. (2005) $F_1F_0$-ATP synthase complex interactions *in vivo* can occur in the absence of the dimer specific subunit e. *J. Bioenerg. Biomembr.* **37,** 55–66
47. Fronzes, R., Weimann, T., Vaillier, J., Velours, J., and Brèthes, D. (2006) The peripheral stalk participates in the yeast ATP synthase dimerization independently of e and g subunits. *Biochemistry* **45,** 6715–6723
48. Velours, J., Stines-Chaumeil, C., Habersetzer, J., Chaignepain, S., Dautant, A., and Brèthes, D. (2011) Evidence of the proximity of ATP synthase subunits 6 (*a*) in the inner mitochondrial membrane and in the supramolecular forms of *Saccharomyces cerevisiae* ATP synthase. *J. Biol. Chem.* **286,** 35477–35484

# Channel Formation by Yeast F-ATP Synthase and the Role of Dimerization in the Mitochondrial Permeability Transition

Michela Carraro, Valentina Giorgio, Justina Sileikyte, Geppo Sartori, Michael Forte, Giovanna Lippe, Mario Zoratti, Ildikò Szabò and Paolo Bernardi

*J. Biol. Chem. 2014, 289:15980-15985.*
*doi: 10.1074/jbc.C114.559633 originally published online May 1, 2014*

---